Inorganic Chemistry

Article

pubs.acs.org/IC

Ba and Sr Binary Phosphides: Synthesis, Crystal Structures, and Bonding Analysis

Juli-Anna Dolyniuk,[†] Hua He,[‡] Alexander S. Ivanov,[§] Alexander I. Boldyrev,*[,§] Svilen Bobev,*[,‡] and Kirill Kovnir*[,†]

[†]Department of Chemistry, University of California—Davis, One Shields Avenue, Davis, California 95616, United States

[‡]Department of Chemistry and Biochemistry, University of Delaware, 304A Drake Hall, Newark, Delaware 19716, United States

[§]Department of Chemistry and Biochemistry, Utah State University, 0300 Old Main Hill, Logan, Utah 84322, United States

Supporting Information

ABSTRACT: Synthesis, crystal structures, and chemical bonding are reported for four binary phosphides with different degrees of phosphorus oligomerization, ranging from isolated P atoms to infinite phosphorus chains. Ba_3P_2 = $Ba_4P_{2.67}\square_{0.33}$ ($\square$ = vacancy) crystallizes in the anti-Th_3P_4 structure type with the cubic space group $I\bar{4}3d$ (no. 220), Z = 6, a = 9.7520(7) Å. In the Ba_3P_2 crystal structure, isolated P^{3-} anions form distorted octahedra around the Ba^{2+} cations. β-Ba_5P_4 crystallizes in the Eu_5As_4 structure type with the orthorhombic space group $Cmce$ (no. 64), Z = 4, a = 16.521(2) Å, b = 8.3422(9) Å, c = 8.4216(9) Å. In the crystal structure of β-Ba_5P_4, one-half of the phosphorus atoms are condensed into P_2^{4-} dumbbells. SrP_2 and BaP_2 are isostructural and crystallize in the monoclinic space group $P2_1/c$ (no. 14), Z = 6, a = 6.120(2)/6.368(1) Å, b = 11.818(3)/12.133(2) Å, c = 7.441(2)/7.687(2) Å, β = 126.681(4)/126.766(2)° for SrP_2/BaP_2. In the crystal structures of SrP_2 and BaP_2, all phosphorus atoms are condensed into $_\infty{}^1P^{1-}$ cis−trans helical chains. Electronic structure calculations, chemical bonding analysis via the recently developed solid-state adaptive natural density partitioning (SSAdNDP) method, and UV−vis spectroscopy reveal that SrP_2 and BaP_2 are electron-balanced semiconductors.

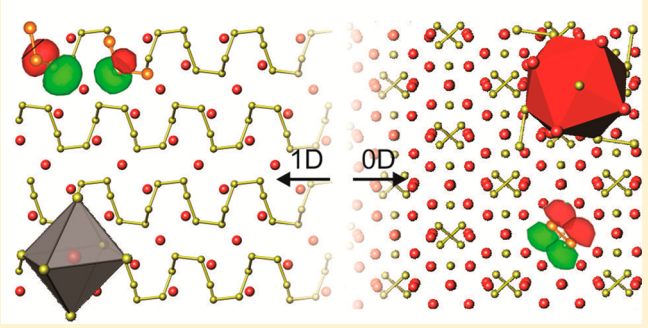

INTRODUCTION

The existence of their unique structural features and properties has led to the enhanced study of polyphosphides in recent years.[1−3] Though studies into these systems began well over 100 years ago, new binary phosphides are still being discovered and characterized to this day.[4−7] The continual discovery of new multicomponent phosphide structures with varying levels of complexity (0D to 3D systems) suggests these systems could be a nearly untapped resource for selective structural tuning and engineering with the goal of obtaining desired properties for applications in the fields of Li- and Na-ion batteries, catalysis, thermoelectrics, magnetic and spintronic materials, etc.[1,2,8−14] This, however, requires a strong fundamental understanding of the structure and chemical bonding in simple binary systems.

In this paper, we report the characterization of four new binary phosphides, one with Sr (SrP_2) and three with Ba (BaP_2, β-Ba_5P_4, and Ba_3P_2). Though all four were referenced by von Schnering et al. in their 1988 polyphosphides review,[1] no crystal structures were ever reported. SrP_2 and BaP_2 are isostructural 1D systems, β-Ba_5P_4 is a newly discovered polymorph of the previously published low-temperature phase α-Ba_5P_4,[15] and Ba_3P_2 is stoichiometrically similar to the known Ba_4P_3[16] but shows a P deficiency of approximately 11%, which leads to a completely different structure type. Single-crystal and powder X-ray diffraction, differential scanning calorimetry, and UV−vis spectroscopy are used in combination with electronic structure and chemical bonding calculations to characterize these new binary phosphides. Chemical bonding is analyzed by means of the recently developed solid-state adaptive natural density partitioning (SSAdNDP) method[17] which allows for performing a molecular orbital type of bonding analysis in extended structures.

EXPERIMENTAL AND THEORETICAL METHODS

Experimental Section. All manipulations with the initial materials and sample handling were performed inside an argon-filled glovebox ($p(O_2) \leq 1$ ppm). The starting materials, metallic barium (Sigma-Aldrich, 99.9%), metallic strontium (Sigma-Aldrich, 99.9%), metallic lead granules (Alfa Aesar, 99.999%), and red phosphorus (Alfa Aesar, 99%), were used as received. Single crystals of BaP_2, Ba_5P_4, and Ba_3P_2 were initially encountered as minor products of reactions aimed at optimizing the synthesis of $Ba_3Ga_3P_5$[11] and to synthesize the hitherto elusive phase $Ba_3In_3P_5$. Those reactions included the elements Ba, Ga (or In), P, and an excess amount of Pb, intended as a flux, to facilitate crystal growth. The mixtures were placed in alumina crucibles, which

Received: June 4, 2015
Published: August 13, 2015

DOI: 10.1021/acs.inorgchem.5b01253
Inorg. Chem. 2015, 54, 8608−8616

Table 1. Data Collection and Structure Refinement Parameters for SrP_2, BaP_2, Ba_5P_4, and Ba_3P_2[a]

empirical formula	SrP_2	BaP_2	Ba_5P_4	$Ba_4P_{2.67}$ (= Ba_3P_2)
CSD no.	429731	429732	429733	429734
fw	149.56 g/mol	199.28 g/mol	810.58 g/mol	632.05 g/mol
temp (K)	200(2)	200(2)	200(2)	200(2)
radiation, λ	Mo Kα, 0.71073 Å	Mo Kα, 0.71073 Å	Mo Kα, 0.71073 Å	Mo Kα, 0.71073 Å
cryst syst	monoclinic	monoclinic	orthorhombic	cubic
space group, Z	$P2_1/c$ (no. 14), 6	$P2_1/c$ (no. 14), 6	$Cmce$ (no. 64), 4	$I\bar{4}3d$ (no. 220)[b], 4
a (Å)	6.120(2)	6.368(1)	16.521(2)	9.7520(7)
b (Å)	11.818(3)	12.133(2)	8.3422(9)	
c (Å)	7.441(2)	7.687(2)	8.4216(9)	
β (deg)	126.681(4)	126.766(2)		
V (Å^3)	431.6(2)	475.8(2)	1160.6(2)	927.4(1)
ρ_{calcd} (g/cm^3)	3.45	4.17	4.64	4.53
μ (cm^{-1})	19.5	13.2	17.2	17.1
no. of measured reflns	5710	6297	7458	3295
no. of unique reflns/R_{int}	1069/0.075	1190/0.034	749/0.079	194/0.041
goodness-of-fit on F^2	1.049	1.057	1.070	1.264
R_1 ($I > 2\sigma_I$)[c]	0.043	0.017	0.027	0.016
wR_2 ($I > 2\sigma_I$)[c]	0.103	0.037	0.041	0.030
R_1 (all data)[c]	0.058	0.018	0.037	0.017
wR_2 (all data)[c]	0.111	0.038	0.046	0.030
largest diff. peak/hole (e$^-$/Å^{-3})	1.93/−1.84	0.56/−0.74	1.32/−1.24	0.66/−0.32

[a]Further details of the crystal structure determination may be obtained from Fachinformations-zentrum Karlsruhe, D-76344 Eggenstein-Leopoldshafen, Germany, by quoting the corresponding depository CSD numbers. [b]Noncentrosymmetric space group. Absolute structure was determined according to the refined Flack parameter of 0.03(9). [c]$R_1 = \sum||F_o| - |F_c||/\sum|F_o|$; $wR_2 = [\sum[w(F_o^2 - F_c^2)^2]/\sum[w(F_o^2)^2]]^{1/2}$, where $w = 1/[\sigma^2F_o^2 + (AP)^2 + (BP)]$, and $P = (F_o^2 + 2F_c^2)/3$; A, B = weight coefficients.

were then jacketed in evacuated fused-silica tubes. The temperature was changed as follows: (1) heat to 1233 K at a rate of 60 K/h, (2) anneal at 1223 K for 40 h, and, subsequently, (3) cool down to 773 K over 16 h (30 K/h rate). The reactions were then taken out of the furnace, and the Pb flux was removed by centrifugation. All samples were dark gray to black small crystals which were found to be air and moisture sensitive. Single crystals of each sample were picked out in the glovebox, and their crystal structures were determined by single-crystal X-ray diffraction. Subsequent to the structural work, which suggested all three samples were binary phases, the reactions were repeated without any Ga or In, following the same method detailed above with adjusted Ba:P ratios dependent on the desired outcome. In all cases, a slight excess of red phosphorus was required, likely due to losses of P from evaporation or due to the solubility of P in Pb. Of the possible Sr analogs, SrP_2, Sr_5P_4, and Sr_3P_2, only the former was successfully obtained from a Pb-flux reaction. Since europium is often divalent and in such a state it maintains an atomic size close to that of Sr, attempts were also made to synthesize EuP_2, Eu_5P_4, and Eu_3P_2, though they proved unsuccessful.

Samples were also prepared by solid-state reactions without flux. Single-phase samples of both SrP_2 and BaP_2 were formed by stoichiometric solid-state reactions of the elements. Two synthetic methods were successful. In the first, large-scale 1 g samples were synthesized by placing the starting materials in glassy carbon crucibles which were subsequently jacketed in evacuated fused-silica ampules. These samples were heated over 17 h to 1073 K and annealed at this temperature for 350 h. Smaller scale samples of 300 mg quantities were synthesized at 1123 K in carbonized, evacuated silica ampules. The latter were ramped over 17 h and annealed for 140 h.

X-ray Powder Diffraction. The SrP_2 and BaP_2 samples were characterized by powder X-ray diffraction (XRD) using a Rigaku Miniflex 600 diffractometer employing Cu Kα radiation (Figure S3) using Be air-free holders. The crystals and polycrystalline powders of Ba_5P_4 and Ba_3P_2 were extremely air sensitive and not amenable to additional characterization. The quick decomposition of all new phosphide samples in ambient air was evident by the abrupt change from a dark-gray to a pale-orange color.

Solid-State UV−vis Spectroscopy. Solid-state UV−vis spectroscopy (Thermo Scientific Evolution 220 Spectrometer) was employed for experimental band gap determinations of SrP_2 and BaP_2 samples. For UV−vis measurements, solid samples were ground into powder and heat sealed in polyethylene bags inside an argon-filled glovebox.

Differential Scanning Calorimetry. A Netzsch differential scanning calorimeter (DSC) was used to characterize the thermal behavior of SrP_2 and BaP_2. In order to maintain similar conditions to those of actual syntheses, DSC measurements were run using small evacuated and sealed silica ampules with enough sample to cover the base of the ampule (approximately 30−50 mg). The samples were initially heated to 673 K at a rate of 10 K/min, and then the heating was slowed to 5 K/min over the 673−1273 K range. A similar cooling scheme was employed. Powder X-ray diffraction was subsequently used to determine the products of DSC thermal treatment.

Single-Crystal X-ray Diffraction. Data for SrP_2, BaP_2, Ba_5P_4, and Ba_3P_2 were collected at 200 K using a Bruker AXS SMART diffractometer with an APEX CCD detector. All four crystals came from flux reactions. The data sets were gathered in batch runs with ω scans of 0.4° step widths and exposure times of 8−12 s per frame. The raw data were integrated with the Bruker SAINT software package. Multiscan absorption corrections were applied, and the solutions and refinements of crystal structures were carried out using the SHELX suite of programs.[18] The data sets for SrP_2 and BaP_2 were readily indexed in similar primitive monoclinic unit cells. Systematic extinctions indicated $P2_1/n$ (no. 14) as the only possible space group for both compounds. After solving both structures in the $P2_1/n$ space group, using the Structure Tidy software, the structures were converted to the standard setting, $P2_1/c$, using the transformation matrix [−1 0 0; 0−1 0; 1 0 1]. The data sets for Ba_5P_4 and Ba_3P_2 were also uniquely indexed in base-centered orthorhombic and body-centered cubic unit cells, respectively. Systematic extinctions indicated $Cmce$ (no. 64) for the former and $I\bar{4}3d$ (no. 220) for the latter as the only possible space groups. Direct methods were successful in solving all four structures, yielding all atomic positions. The initial refinement cycles proceeded smoothly (except for the Ba_3P_2 = $Ba_4P_{2.67}$ structure, where convergence was achieved only after refining the occupation factor of the P site). The final refinements were performed using

DOI: 10.1021/acs.inorgchem.5b01253
Inorg. Chem. 2015, 54, 8608−8616

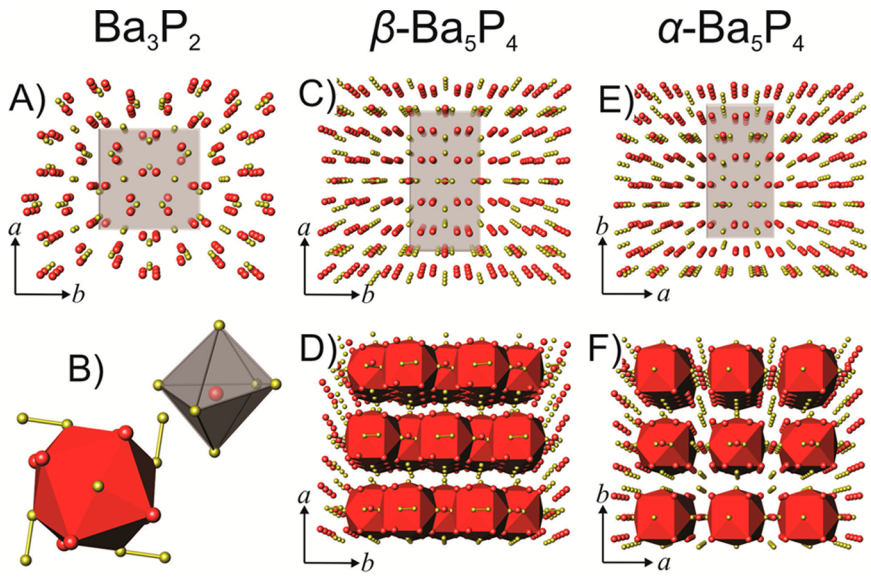

Figure 1. Crystal structures of $Ba_4P_{2.67}$ = Ba_3P_2 (A), β-Ba_5P_4 (C), and α-Ba_5P_4 (E). Ba atoms are shown in red, and P atoms are shown in gold. (D and F) Capped, cube-like coordinations of Ba atoms in both β-Ba_5P_4 and α-Ba_5P_4 structures, respectively. An enlarged Ba coordination cube is shown in B along with a representation of the distorted octahedron Ba@P_6 present in the crystal structure of Ba_3P_2. Note: Ba_3P_2 is shown with fully occupied P positions, i.e., Ba_4P_3.

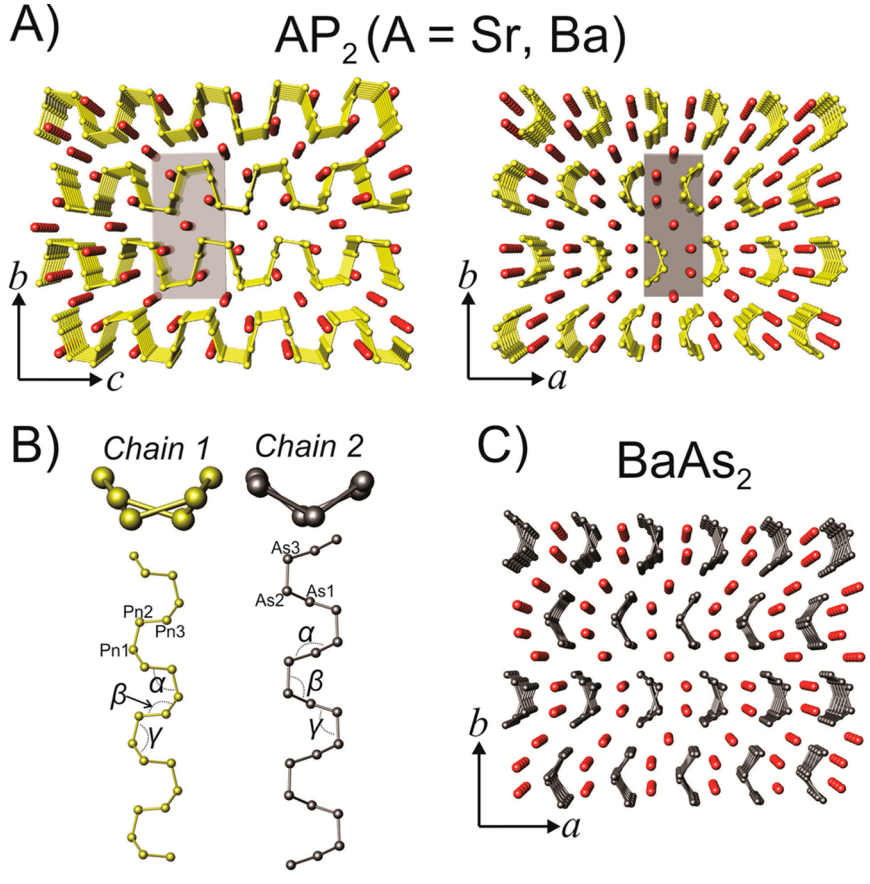

Figure 2. Crystal structures of (A) SrP_2 and BaP_2 and (C) $BaAs_2$. Ba/Sr, red; P, yellow; As, black. There are two types of As chains in the structure of $BaAs_2$ (B), while only chains of type 1 are present in the structures of Ba and Sr diphosphides.

anisotropic atomic displacement parameters for all atoms. A summary of pertinent information relating to unit cell parameters, data collection, and refinements is provided in Table 1.

The structures of SrP_2 and BaP_2 were also confirmed by refinements from crystals obtained via stoichiometric solid-state reactions. Data for both SrP_2 and BaP_2 were collected at 90 K using a Bruker AXS SMART diffractometer with an APEX-II CCD detector. Unit cell constants, atomic positions, and refined distances/angles are in excellent agreement with the data for flux-synthesized crystals. The details, in the form of CIFs, are provided as Supporting Information.

DOI: 10.1021/acs.inorgchem.5b01253
Inorg. Chem. 2015, 54, 8608−8616

Quantum-Chemical Calculations. The electronic structure calculations and bonding analyses were carried out using the tight binding, linear muffin-tin orbital, atomic sphere approximation (TB-LMTO-ASA) program. The Barth–Hedin exchange potential was employed for the LDA calculations. The radial scalar-relativistic Dirac equation was solved to obtain the partial waves. A basis set containing Sr(5s,4d), Ba(6s,5d,4f), and P(3s,3p) orbitals was employed for the self-consistent calculation, with downfolded Sr(5p), Ba(6p), and P(3d) functions. The density of states (DOS) and band structures were calculated after convergence of the total energy on a dense k mesh of 16 × 8 × 16 points, with 650 irreducible k points.

Chemical bonding analyses of the SrP_2, BaP_2, and Ba_5P_4 Zintl phase systems were performed using the solid-state adaptive natural density partitioning (SSAdNDP) method[17]—an extended version of the AdNDP method,[19] which has successfully been employed to analyze the chemical bonding of the LiP[6] and Na_8BaSn_6[17] Zintl phases, as well as mixed phosphorus–carbon clusters,[20] porphyrinoids,[21] hexaphosphabenzene (P_6) containing triple-decker sandwich complexes,[22] and hypervalent iodine reagents.[23] Both methods (AdNDP and SSAdNDP) are extensions of the natural bonding orbital (NBO) method developed for molecules by Foster and Weinhold[24] and for periodic systems by Dunnington and Schmidt.[25] SSAdNDP analyzes the first-order reduced density matrix in order to obtain its local block eigenfunctions with optimal convergence properties for an electron density description. The obtained local blocks correspond to the sets of n atoms (n ranging from 1 to the total number of atoms in the molecule) that are tested for the presence of two-electron objects (n-center two electron (nc-2e) bonds, including core electrons and lone pairs as a special case of n = 1) associated with this particular set of n atoms. SSAdNDP initially searches for core electron pairs and lone pairs (1c-2e), then 2c-2e, 3c-2e, ..., and finally nc-2e bonds. At every step, the density matrix is depleted of the density corresponding to the appropriate bonding elements. SSAdNDP accepts only those bonding elements whose occupation numbers (ONs) exceed the specified threshold values, which are usually chosen to be close to 2.00 |e|. Thus, the SSAdNDP method recovers both Lewis bonding elements (1c-2e and 2c-2e objects, corresponding to the core electrons and lone pairs, and two-center two-electron bonds) and delocalized bonding elements. In SSAdNDP, a projection algorithm is used to obtain a representation of the delocalized plane wave density functional theory (PW DFT) results in a localized atomic orbital (AO) basis. As long as an appropriate AO basis set is chosen (it is usually trimmed of any functions with angular momentum $l \geq 4$ as well as diffuse functions with exponents < 0.1), the projection is found to result in an accurate density matrix.[25] In the current study, the def2-SVP basis set[26] was used to represent the projected PW density using 3 × 6 × 3 (SrP_2 and BaP_2) and 6 × 3 × 3 (Ba_5P_4) k-point grids. This basis set was selected so that, on average, less than 1% of the density of each occupied plane wave band was lost in projecting into the AO basis to guarantee that the density matrix used in the SSAdNDP procedure accurately represents the original plane-wave results. Plane-wave DFT calculations were performed using the Vienna ab initio simulations package (VASP, version 4.6)[27] with PAW pseudopotentials from the VASP database[28] and the PBE density functional.[29] The default plane-wave cutoff energy of the associated pseudopotential was used. The Brillouin zone was sampled with a Γ-centered Monkhorst–Pack grid.[30] The Visualization for Electronic and Structural Analysis software (VESTA, series 3) was used for visualization of chemical bonding.[31]

RESULTS AND DISCUSSION

Synthesis. BaP_2 together with SrP_2 had been previously mentioned by Hönle and von Schnering in their 1988 polyphosphides review, but their syntheses and crystal structures were never reported.[1] SrP_2 and BaP_2 were successfully synthesized in high yields, either by Pb-flux reactions or from the elements by direct solid-state reactions, as described in the Experimental Section. Other metals were also tried, such as fluxes (Ga, In, Sn, Zn), but such experiments preferentially formed ternary phases. DSC experiments in evacuated silica tubes indicate that both AP_2 phases melt congruently at 1053(10) (BaP_2) and 1123(10) K (SrP_2). Powder XRD analysis of the samples treated by DSC seems to confirm the recrystallization of the melts into the original AP_2 phases, though analysis of air-sensitive DSC products was hampered by small sample size.

The same polyphosphides review paper[1] also mentions several other known binary phases in the Ba–P phase diagram, including Ba_3P_2. This cubic compound with the anti-Th_3P_4 structure type is P deficient (e.g., $Ba_4P_{2.67}$), as per earlier work by Maass[32] and Hadenfeldt.[33] From the earlier synthetic work

Table 2. Selected Angles in the $_\infty{}^1Pn^{1-}$ Helical Chains in Crystal Structures of SrP_2, BaP_2, and $BaAs_2$[a]

	SrP_2	BaP_2	$BaAs_2$ chain 1	$BaAs_2$ chain 2
α Pn1–Pn3–Pn2 (deg)	111.50(12)	113.446(5)	118.7	110.5
β Pn3–Pn2–Pn1 (deg)	110.41(13)	110.08(4)	108.4	103.8
γ Pn2–Pn1–Pn3 (deg)	108.36(12)	111.50(4)	108.0	109.9
Pn3–Pn2–Pn1–Pn3 (deg)	38.1	33.6	39.3	105.1
Pn1–Pn3–Pn2–Pn1 (deg)	113.3	113.5	119.2	13.4
Pn2–Pn1–Pn3–Pn2 (deg)	86.4	90.2	80.3	96.6
average P–P (Å)	2.22	2.23		
shortest A–P (Å)	3.029(2)	3.227(1)		
shortest A–A (Å)	4.016(1)	4.2024(7)	4.1641	

[a] $BaAs_2$ crystal structure was reported at 245 K,[41] while SrP_2 and BaP_2 data are from 200 K single-crystal experiments.

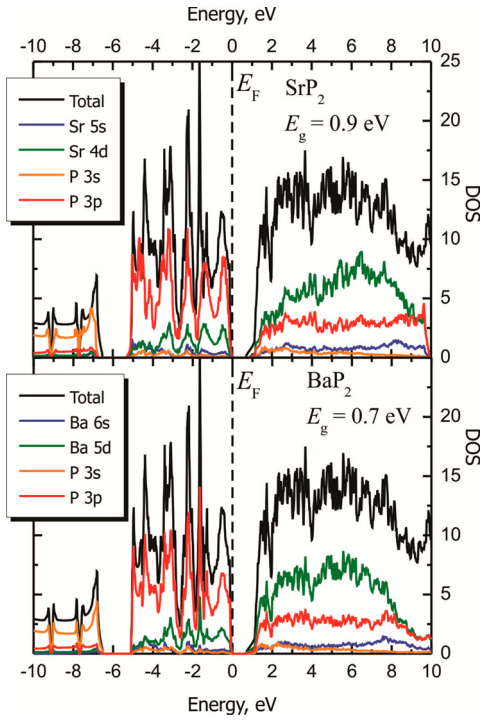

Figure 3. Density of states (DOS) diagram for (top) SrP_2 and (bottom) BaP_2. The contributions from Sr(5s)/Ba(6s), Sr(4d)/Ba(5d), P(3s), and P(3p) are shown in blue, green, orange, and red, respectively.

DOI: 10.1021/acs.inorgchem.5b01253
Inorg. Chem. 2015, 54, 8608–8616

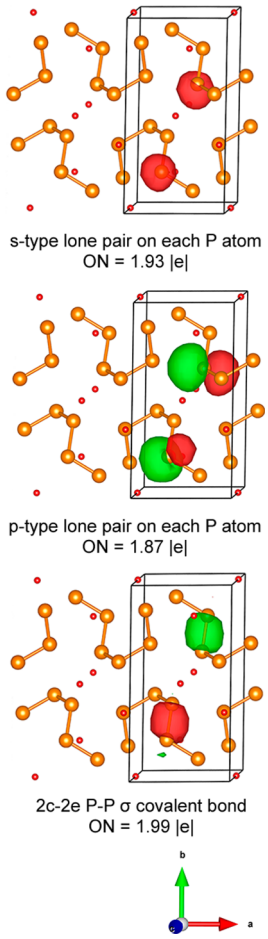

Figure 4. SSAdNDP chemical bonding pattern for SrP_2. The isovalue is 0.05 au; ON stands for occupation numbers. All bonding elements are visualized for only two P atoms in the unit cell. Color scheme: Sr, red; P, orange. Sr spheres were minimized for clarity.

Table 3. SSAdNDP and NBO Results for the SrP_2 System

SSAdNDP	occupancy |e|	center (bond % polarization)	NBO, hybridization (function, %)
P–P σ bond	1.99	P (50)	*s* 20, *p* 80
		P (50)	*s* 20, *p* 80
P–P σ* antibond	0.17	P (50)	*s* 20, *p* 80
		P (50)	s 20, *p* 80
P LP(1)–*s* type	1.93	P (100)	*s* 62, *p* 38
P LP(2)–*p* type	1.87	P (100)	*s* 02, *p* 98

and from the herein described reactions with metal fluxes, one must conclude that the line compound Ba_3P_2 is also a thermodynamically stable phase in the Ba–P phase diagram, which is accessible by a variety of synthetic methods.

The last point of discussion concerns Ba_5P_4. Hönle and von Schnering do not list Ba_5P_4 in their review, but a compound with the same chemical makeup, dubbed α-Ba_5P_4, was reported in 2003 by Belin and co-workers.[15] α-Ba_5P_4 was structurally characterized and assigned the Sm_5Ge_4 structure type (space group *Pnma*), and the paper touches on the possibility of dimorphism in the system, similar to the dimorphism in the "5–4" rare-earth metal germanides and stannides.[34] The 2003 report briefly refers to a dissertation from 1989,[35] citing the

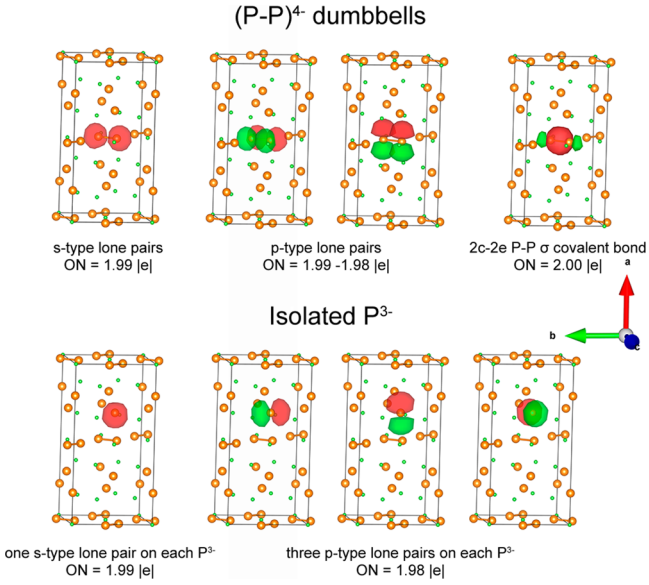

Figure 5. SSAdNDP chemical bonding pattern for Ba_5P_4. The isovalue is 0.03 au; ON stands for occupation numbers. All bonding elements are visualized for only one P_2^{4-} dumbbell and one isolated P^{3-} anion in the unit cell. Color scheme: Ba, green; P, orange. Ba spheres were minimized for clarity.

Table 4. SSAdNDP and NBO Results for the Ba_5P_4 System

SSAdNDP	occupancy |e|	center (bond % polarization)	NBO, hybridization (function, %)
P–P σ bond (dumbbell)	2.00	P (50)	*s* 20, *p* 80
		P (50)	*s* 20, *p* 80
P–P σ* antibond (dumbbell)	0.40	P (50)	*s* 20, *p* 80
		P (50)	*s* 20, *p* 80
P (dumbbell) LP(1)–*s* type	1.98	P (100)	*s* 85, *p* 15
P (dumbbell) LP(2)–*p* type	1.98	P (100)	*s* 0, *p* 100
P (dumbbell) LP(3)–*p* type	1.99	P (100)	*s* 0, *p* 100
P (isolated) LP(4)–*s* type	1.99	P (100)	*s* 93, *p* 7
P (isolated) LP(5)–*p* type	1.98	P (100)	*s* 7, *p* 93
P (isolated) LP(6)–p type	1.98	P (100)	*s* 0, *p* 100
P (isolated) LP(7)–*p* type	1.98	P (100)	*s* 0, *p* 100

existence of β-Ba_5P_4 (Eu_5As_4 structure type, space group *Cmce*). The Inorganic Crystal Structure Database, accessed in April 2015,[36] however, does not indicate that the crystal structure of β-Ba_5P_4 has been established to date.

Crystal Structures. We begin the discussion with the simplest and most recognizable structure of the three, that of $Ba_4P_{2.67}$, which was also referred to as Ba_3P_2. This phase, as described in earlier papers,[32,33] belongs to the anti-Th_3P_4 structure type (Pearson symbol *cI*28) with the cubic space group $I\bar{4}3d$ (no. 220). The structure can be viewed as a complex arrangement of isolated P^{3-} anions, forming distorted octahedra around the Ba^{2+} cations (Figures 1 and S1). Each P^{3-} anion is coordinated by eight cations, and there are no anion–anion bonding contacts. We also note that this is the inverse Th_3P_4 structure, i.e., the Ba^{2+} cations take the P site (Wyckoff

DOI: 10.1021/acs.inorgchem.5b01253
Inorg. Chem. 2015, 54, 8608–8616

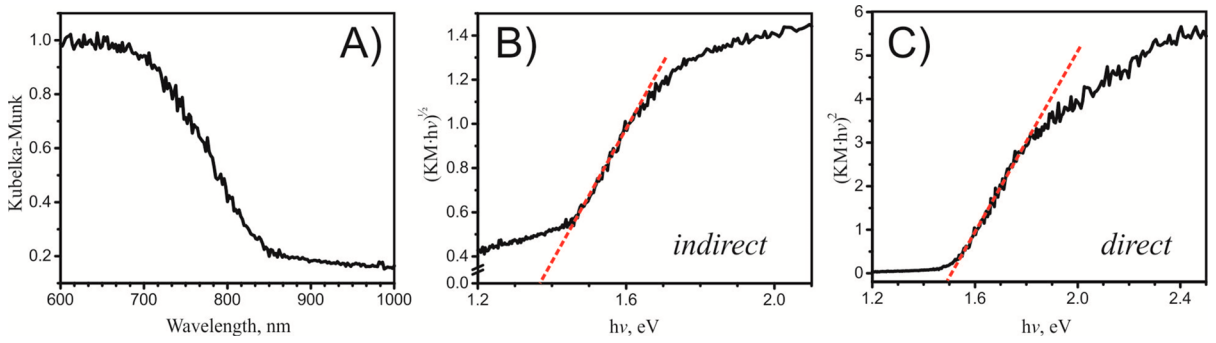

Figure 6. Solid-state UV−vis spectra of SrP_2: (A) Kubelka−Munk diffuse reflectance; Tauc plots for allowed (B) indirect and (C) direct transitions.

index 16*c*), and the P^{3-} anions occupy the Th site (Wyckoff index 12*a*). The structure follows valence rules by virtue of leaving 1/9 of the P^{3-} anions randomly missing. A stoichiometric Ba_4P_3 with this structure would be electron deficient, since there are only 8 electrons provided by the cations, while three P^{3-} anions will require 9 electrons to complete their octets. The crystal structure and electronic structure of the isotypic and isoelectronic Ba_3As_2 have also been detailed in an earlier paper.[37] Our structural work (Table 1, a = 9.7520(7) Å at 200 K) is in excellent agreement with the earlier room-temperature work by Maass (a = 9.775 Å)[32] and Hadenfeldt (a = 9.779 Å).[33] An accurate refinement of the occupation factor of the P site from single-crystal data shows that, when freed, it is 86.2(2)%, confirming the notion that all phosphides and arsenides with this structure (with divalent cations) are substoichiometric but electron-precise Zintl phases.

We also would like to mention that a stoichiometric Ba_4P_3 compound is known;[16] however, its structure is very different from the one discussed above, and it contains polymeric P anions. The crystal structure of Ba_3P_2 is shown in Figure 1. A graphical comparison of the Ba_3P_2 ($Ba_4P_{2.67}$) and stoichiometric Ba_4P_3 structures are provided as Supporting Information in Figure S1.

A higher level of structural complexity is realized in Ba_5P_4 (Eu_5As_4 or $Tm_5Si_2Sb_2$ structure type, Pearson symbol *oC*36, space group *Cmce*). In this crystal structure, phosphorus atoms are in a formally less reduced state, whereby one-half of the phosphorus atoms in the structure are dimerized (Figure 1).

The phase is apparently dimorphic, since α-Ba_5P_4 (Sm_5Ge_4 structure type, space group *Pnma*) is known to exist.[15] On the basis of the observation that α-Ba_5P_4 was obtained from a stoichiometric melt cooled to room temperature while β-Ba_5P_4 was the product of a flux reaction quenched at 773 K, the earlier assignment of low-temperature and high-temperature modifications appears correct. Also, since we were able to isolate β-Ba_5P_4 from flux reactions only, it is reasonable to expect that α-Ba_5P_4 is the thermodynamically more stable product, while β-Ba_5P_4 is the faster growing albeit less stable phase. This conjecture, however, is merely a speculation at this point, and more structural/thermal analysis work is needed to resolve the phase equilibria in the Ba−P phase diagram at 55.6 atom % Ba.

The structure of β-Ba_5P_4 (a = 16.521(2) Å; b = 8.3422(9) Å; c = 8.4216(9) Å; V = 1160.6(2) Å^3, space group *Cmce*) can be viewed as a more symmetric version of α-Ba_5P_4. Interestingly, it has orthorhombic symmetry similar to the α-phase, which shows similar unit cell constants (a = 8.330 Å; b = 16.503 Å; c = 8.405 Å; V = 1155.4 Å^3)[15] but crystallizes in the space group *Pnma*. β-Ba_5P_4 has 4 crystallographically unique positions in the asymmetric unit (two Ba and two P atoms), while α-Ba_5P_4 has 6 crystallographically unique positions in the asymmetric unit (three Ba and three P atoms). Put simply, regardless of small changes in the local coordination, the two structures have the same fraction, 50%, of P atoms forming P−P bonds. In both structures two separate fragments can be distinguished: slabs of condensed trigonal prisms of Ba atoms and slabs of Ba trigonal prisms fused with Ba cubes. All prisms are centered by P atoms, while all "cubes" are centered by Ba atoms (Figure 1). The structure can also be visualized as an intergrowth of Mo_2FeB_2-type[38] and FeB-type[39] fragments. The Mo_2FeB_2 structure, in turn, can be seen as a structure made up of CsCl-like cubes and AlB_2-like trigonal prisms (see Supporting Information Figure S2 for the visualization of the structure according to this parlance).

The P−P bonds are formed by the P(2) atoms and are 2.325(5) Å long. With the Pauling covalent radius for P as 1.10 Å,[40] these bonds are slightly longer than a single-bonded P_2 dumbbell. For comparison, the P−P bonds in α-Ba_5P_4 are 2.304(6) Å, and the P−P bonds within the ${}_\infty{}^1P^{1-}$ chain in BaP_2 fall into the range of 2.196(1) to 2.251(1) Å.

SrP_2 and BaP_2 crystallize in the same primitive monoclinic space group, $P2_1/c$, Pearson symbol *mP*18 (Figure 2). AP_2 are similar in structure to $BaAs_2$,[41] consisting of ${}_\infty{}^1Pn^{1-}$ helical chains packed in between layers of A cations (A = Sr, Ba). In the structure of $BaAs_2$, two different types of cis-trans helical As chains are present (Figure 2c).[41]

The crystal structures of AP_2 are different than $BaAs_2$ in that only one type of P chain is present in their crystal structure; this type chain is a P analogue of the chain 1 present in $BaAs_2$. The ${}_\infty{}^1P^{1-}$ chains are common structural components of polyphosphides and polyarsenides.[1−3,6,42] A high flexibility of these chains is achieved as a result of the variations in dihedral angles, allowing them to accommodate various alkaline, alkaline-earth, rare-earth, and transition metal cations as well as group 12 and 14 elements such as Zn, Cd, Hg, Si, and Ge. Recent computational work predicts the possibility of such chains forming a nanotoroid ring.[43]

Selected angles and distances for AP_2 and, for comparison, $BaAs_2$,[41] are shown in Table 2. The β angles (∠Pn3−Pn2−Pn1) for AP_2 are very similar, while the other two angles, α and γ, are slightly larger in BaP_2 than in SrP_2. This suggests the ${}_\infty{}^1P^{1-}$ chains in BaP_2 are to some extent modified to accommodate the larger Ba cations in BaP_2 versus the smaller Sr cations in SrP_2. Similarly, the dihedral angles ∠Pn1−Pn3−Pn2−Pn1 for both SrP_2 and BaP_2 are nearly identical. The local coordination of one of the A cations in the AP_2 crystal structure is very close to the coordination found in the Ba_3P_2 crystal

DOI: 10.1021/acs.inorgchem.5b01253
Inorg. Chem. 2015, 54, 8608−8616

structure: those cations are surrounded by 6 P atoms forming nearly regular octahedra (Figure S4).

Both AP_2 structures exhibit almost identical P−P bond distances in the range of 2.20−2.25 Å. This is within the range of single covalent P−P bond distances. This indicates that the accommodation of different sized cations, such as Sr and Ba, is achieved mainly due to the modification of dihedral and bond angles in the $_\infty{}^1P^{1-}$ helical chains, while the interatomic distances remain almost unchanged. The shortest A−A and A−P distances are approximately 0.2 Å longer in BaP_2 than in SrP_2 (Table 2).

Electronic Structure. According to the Zintl concept,[44] all four binary phosphides that are the subject of this paper, SrP_2, BaP_2, Ba_3P_2, and Ba_5P_4, are valence compounds. Ba_3P_2, whose structure features isolated P^{3-} anions, can be represented as $(Ba^{2+})_3(P^{3-})_2$. Ba_5P_4, whose structure features isolated P^{3-} anions and isolated P_2^{4-} dumbbells, can be considered $(Ba^{2+})_5(P_2^{4-})_1(P^{3-})_2$. The phosphorus atoms in the SrP_2 and BaP_2 polyphosphides form two covalent bonds to other phosphorus atoms and hold two electron lone pairs. Such phosphorus atoms need 6 electrons, i.e., they are formally P^{1-}. This implies that SrP_2 and BaP_2 can be represented as $A^{2+}(P^{1-})_2$, where A^{2+} stands for Sr^{2+} or Ba^{2+}. According to the band structure calculations by the LMTO method (Figure 3), SrP_2 and BaP_2 are semiconductors with E_g = 0.9 and 0.7 eV, respectively. P(3p) and Sr(4d)/Ba(5d) orbitals are the main contributors to the top of the valence band and to the bottom of the conduction band. More detailed bonding analysis was performed with the SSAdNDP method.

Chemical Bonding. To clarify the chemical bonding of phosphorus polyanions in the SrP_2 and BaP_2 Zintl phases, we performed solid-state adaptive natural density (SSAdNDP) analysis.[17] SSAdNDP, which is an extension of the periodic NBO method,[25] interprets chemical bonding in systems with translational symmetry in terms of classical lone pairs and two-center bonds, as well as multicenter delocalized bonding. Essentially, SSAdNDP is a very efficient and visual approach, allowing us to decompose the complex results of solid-state calculations into a chemically intuitive representation. For SrP_2 the NAO (natural atomic orbital) population analysis implemented in the solid-state NBO program[25] showed P and Sr atoms have a charge of −0.8*e* and +1.6*e*, respectively, confirming the expectation of strong ionic character for Sr−P interactions. Though NBO indicates a small covalent contribution to the Sr−P interaction, with the Sr 4d orbitals' participation [hybridization: Sr (s 51.2%; p 0.21%; d 48.6%) and P (s 1.3%; p 98.7%)], the Sr−P bond is significantly polarized toward the phosphorus atom [polarization: Sr (1.1%) and P (98.9%)] and thus can be regarded as ionic. The SSAdNDP analysis revealed 4 core electron pairs on each Sr atom with an occupation number (ON) of 2.00 |e| (not shown), one *s*-type and one *p*-type lone pair (LP) on each of the P atoms, ON = 1.93 and 1.87 |e|, respectively and 2c-2e σ bonds between P atoms in the phosphorus polyanion chain (Figure 4). NBO analysis also suggests a covalent nature of the P−P bond, which has an occupancy of 1.99 |e|, with a corresponding antibonding occupancy of 0.17 |e|, and lacks polarization toward either P atom, as expected. The *p*-type phosphorus lone pair is oriented perpendicular to the plane containing the P−P covalent bonds. All bonding natural bond orbitals have an almost ideal occupancy, indicating that the simple Zintl description should be a good representation of the complete electron density. The results of SSAdNDP and NBO analyses for SrP_2 are summarized in Table 3. We obtained a similar chemical bonding pattern for the BaP_2 phase (see Table S2 and Figure S5 in Supporting Information for more details) and thus it is not discussed here. Overall, our chemical bonding analyses justify that SrP_2/BaP_2 polyphosphides are typical Zintl phases with compositions that can be written as $(Sr^{2+})(P^{1-})_2$ and $(Ba^{2+})(P^{1-})_2$, respectively.

Chemical bonding analysis for β-Ba_5P_4 showed that the charge distribution (from NAO analysis)[25] is in agreement with the Zintl concept predictions, and it confirms the ionic nature of the interactions between Ba and P atoms in the β-Ba_5P_4 polymorph. SSAdNDP revealed 4 core electron pairs on each Ba atom, ON = 2.00 |e| (not shown), four single covalent 2c-2e σ bonds per unit cell, forming (P−P) dumbbell structures, one *s*-type and two *p*-type lone pairs located on the bonded phosphorus atoms of the $(P-P)^{4-}$ unit, ON = 1.99−1.98 |e|, and one *s*-type and three *p*-type lone pairs, ON = 1.99−1.98 |e|, on each of the isolated P^{3-} phosphorus ions (Figure 5 and Table 4). As can be seen from Table 4, the associated P−P σ antibonds are occupied at 0.40 |e|. The antibond occupancy, donated from phosphorus lone pairs, indicates donor/acceptor interactions between the corresponding Lewis-type and non-Lewis-type (antibonding) orbitals. Thus, the structure of β-Ba_5P_4 should be represented as containing both discrete anions P^{3-} and dumbbells P_2^{4-} separated by Ba^{2+} cations, yielding the corresponding formula: $(Ba^{2+})_5(P^{3-})_2(P_2^{4-})$. As one may see, our SSAdNDP analysis of BaP_2, SrP_2, and β-Ba_5P_4 phases provided a localized and inherently "chemical" representation of bonding in terms of localized Lewis-type objects such as lone pairs and two-center bonds in these periodic systems. Hence, we anticipate that our chemically intuitive SSAdNDP approach will be just as helpful in analyzing the chemical bonding in more complicated phases where the chemical bonding situation is unclear and could be described by localized as well as nonclassical multicenter bonding.

Solid-State UV−vis Spectroscopy. Solid-state UV−vis spectroscopy was employed to determine the experimental band gaps of both SrP_2 and BaP_2. Several samples for each composition were measured. Unfortunately, reliable data for BaP_2 could not be obtained since its absorption onset appeared to be outside the range of the instrument, suggesting a band gap smaller than 1.1 eV. A typical spectrum for SrP_2 is shown in Figure 6a. According to the calculated Tauc plots, SrP_2 exhibits indirect and direct optical transitions corresponding to band gaps of 1.3(1) and 1.5(1) eV, respectively (Figure 6). The experimental band gap is larger than what was predicted by LMTO calculations. While most computational methods lack absolute accuracy in predicting the band gaps of semiconductors, the trends revealed by the calculations are often correct. In this case, the band gap of BaP_2 is smaller than the band gap of SrP_2, as calculated.

■ CONCLUSIONS

The synthesis, features of the crystal and electronic structures, as well as optical properties for four new binary phosphides were explored. The decrease of the Ba/P ratio from 3/2 in Ba_3P_2 to 5/4 in β-Ba_5P_4 to 1/2 in BaP_2 results in the condensation of the isolated phosphorus atoms first to dumbbells (β-Ba_5P_4) and then to infinite phosphorus chains (BaP_2 and SrP_2). According to quantum-chemical calculations and bonding analysis β-Ba_5P_4, BaP_2, and SrP_2 are electron-balanced semiconductors. UV−vis spectroscopy confirms the semiconducting nature of the BaP_2 and SrP_2 compounds.

DOI: 10.1021/acs.inorgchem.5b01253
Inorg. Chem. 2015, 54, 8608−8616

■ ASSOCIATED CONTENT

Supporting Information

The Supporting Information is available free of charge on the ACS Publications website at DOI: 10.1021/acs.inorgchem.5b01253.

Additional crystallographic tables, powder X-ray diffraction patterns, additional structural figures, and complete SSAdNDP chemical bonding analysis for the BaP_2 system (PDF)

Crystallographic information files (CIF)

Crystallographic information file (CIF)

Crystallographic information file (CIF)

Crystallographic information file (CIF)

Crystallographic information file (CIF)

Crystallographic information file (CIF)

■ AUTHOR INFORMATION

Corresponding Authors

*E-mail: a.i.boldyrev@usu.edu. Phone: 435-797-1630.

*E-mail: bobev@udel.edu. Phone: 302-831-8720.

*E-mail: kkovnir@ucdavis.edu. Phone: 530-752-5563.

Author Contributions

The manuscript was written through contributions from all authors. All authors have given approval to the final version of the manuscript

Notes

The authors declare no competing financial interest.

■ ACKNOWLEDGMENTS

We thank Prof. S. M. Kauzlarich for access to the DSC and Prof. F. E. Osterloh for access to the UV−vis spectrometer. Research performed at UC Davis is supported by the U.S. Department of Energy, Office of Basic Energy Sciences, Division of Materials Sciences and Engineering under Award DE-SC0008931. Work at the University of Delaware was supported by the U.S. Department of Energy Office of Science, Office of Basic Energy Sciences, Division of Materials Sciences and Engineering under Award Number DE-SC0008885. Research performed at Utah State University is supported by the National Science Foundation under award CHE-1361413. Computer, storage, and other resources from the Division of Research Computing in the Office of Research and Graduate Studies at Utah State University and the Center for High Performance Computing at the University of Utah are gratefully acknowledged.

■ REFERENCES

(1) von Schnering, H. G.; Hoenle, W. *Chem. Rev.* **1988**, *88*, 243−273.

(2) Pöttgen, R.; Hönle, W.; von Schnering, H. G. In *Encyclopedia of Inorganic Chemistry*, 2nd ed.; King, R. B., Ed.; Wiley: Chichester, U.K., 2005; Vol. *VIII*, pp 4255−4308.

(3) Bawohl, M.; Nilges, T. *Z. Anorg. Allg. Chem.* **2015**, *641*, 304−310.

(4) Dolyniuk, J.; Kaseman, D.; Sen, S.; Zhao, J.; Osterloh, F. E.; Kovnir, K. *Chem. - Eur. J.* **2014**, *20*, 10829−10837.

(5) Schäfer, K.; Benndorf, C.; Eckert, H.; Pöttgen, R. *Dalton Trans.* **2014**, *43*, 12706−12710.

(6) Ivanov, A. S.; Morris, A. J.; Bozhenko, K. V.; Pickard, C. J.; Boldyrev, A. I. *Angew. Chem., Int. Ed.* **2012**, *51*, 8330−8333.

(7) Chen, X.; Zhu, L.-P.; Yamanaka, S. *J. Solid State Chem.* **2003**, *173*, 449−455.

(8) Shatruk, M. M.; Kovnir, K. A.; Shevelkov, A. V.; Popovkin, B. A. *Angew. Chem., Int. Ed.* **2000**, *39*, 2508−2509.

(9) Zaikina, J. V.; Kovnir, K.; Burkhardt, U.; Schnelle, W.; Haarmann, F.; Schwarz, U.; Grin, Yu.; Shevelkov, A. V. *Inorg. Chem.* **2009**, *48*, 3720−3730.

(10) Zaikina, J. V.; Kovnir, K.; Haarmann, F.; Schnelle, W.; Burkhardt, U.; Borrmann, H.; Schwarz, U.; Grin, Yu.; Shevelkov, A. V. *Chem. - Eur. J.* **2008**, *14*, 5414−5422.

(11) He, H.; Tyson, C.; Saito, M.; Bobev, S. *Inorg. Chem.* **2013**, *52*, 499−505.

(12) Makongo, J. P. A.; You, T.-S.; He, H.; Suen, N.-T.; Bobev, S. *Eur. J. Inorg. Chem.* **2014**, *2014*, 5113−5124.

(13) Kovnir, K.; Thompson, C. M.; Zhou, H. D.; Wiebe, C. R.; Shatruk, M. *Chem. Mater.* **2010**, *22*, 1704−1713.

(14) Kovnir, K.; Reiff, W. M.; Menushenkov, A. P.; Yaroslavtsev, A. A.; Chernikov, R. V.; Shatruk, M. *Chem. Mater.* **2011**, *23*, 3021−3024.

(15) Derrien, G.; Tillard, M.; Manteghetti, A.; Belin, C. *Z. Anorg. Allg. Chem.* **2003**, *629*, 1601−1609.

(16) Hadenfeldt, C.; Terschüren, H. U.; Hönle, W.; Schröder, L.; von Schnering, H. G. *Z. Anorg. Allg. Chem.* **1993**, *619*, 843−848.

(17) Galeev, T. R.; Dunnington, B. D.; Schmidt, J. R.; Boldyrev, A. I. *Phys. Chem. Chem. Phys.* **2013**, *15*, 5022−5029.

(18) Sheldrick, G. M. *Acta Crystallogr., Sect. A: Found. Crystallogr.* **2008**, *A64*, 112−122.

(19) Zubarev, D. Y.; Boldyrev, A. I. *Phys. Chem. Chem. Phys.* **2008**, *10*, 5207−5217.

(20) Ivanov, A. S.; Bozhenko, K. V.; Boldyrev, A. I. *J. Chem. Theory Comput.* **2012**, *8*, 135−140.

(21) Ivanov, A. S.; Boldyrev, A. I. *Org. Biomol. Chem.* **2014**, *12*, 6145−6150.

(22) Ivanov, A. S.; Bozhenko, K. V.; Boldyrev, A. I. *Inorg. Chem.* **2012**, *51*, 8868−8872.

(23) Ivanov, A. S.; Popov, I. A.; Boldyrev, A. I.; Zhdankin, V. V. *Angew. Chem., Int. Ed.* **2014**, *53*, 9617−9621.

(24) Foster, J. P.; Weinhold, F. *J. Am. Chem. Soc.* **1980**, *102*, 7211−7218.

(25) Dunnington, B. D.; Schmidt, J. R. *J. Chem. Theory Comput.* **2012**, *8*, 1902−1911.

(26) Weigend, F.; Ahlrichs, R. *Phys. Chem. Chem. Phys.* **2005**, *7*, 3297−3305.

(27) (a) Kresse, G.; Hafner, J. *Phys. Rev. B: Condens. Matter Mater. Phys.* **1993**, *47*, 558−561. (b) Kresse, G.; Hafner, J. *Phys. Rev. B: Condens. Matter Mater. Phys.* **1994**, *49*, 14251−14269. (c) Kresse, G.; Furthmüller, J. *Phys. Rev. B: Condens. Matter Mater. Phys.* **1996**, *54*, 11169−11186. (d) Kresse, G.; Furthmüller, J. *Comput. Mater. Sci.* **1996**, *6*, 15−50.

(28) (a) Blöchl, P. E. *Phys. Rev. B: Condens. Matter Mater. Phys.* **1994**, *50*, 17953−17979. (b) Kresse, G.; Joubert, D. *Phys. Rev. B: Condens. Matter Mater. Phys.* **1999**, *59*, 1758−1775.

(29) (a) Perdew, J. P.; Burke, K.; Ernzerhof, M. *Phys. Rev. Lett.* **1996**, *77*, 3865−3868. (b) Perdew, J. P.; Burke, K.; Ernzerhof, M. *Phys. Rev. Lett.* **1997**, *78*, 1396−1396.

(30) Monkhorst, H. J.; Pack, J. D. *Phys. Rev. B* **1976**, *13*, 5188−5192.

(31) Momma, K.; Izumi, F. *J. Appl. Crystallogr.* **2011**, *44*, 1272−1276.

(32) (a) Maass, K. E. *Z. Anorg. Allg. Chem.* **1970**, *374*, 11−18. (b) Maass, K. E. *Naturwissenschaften* **1968**, *55*, 489−490.

(33) Hadenfeldt, C. *Z. Anorg. Allg. Chem.* **1977**, *436*, 113−121.

(34) Suen, N.-T.; Bobev, S. *Z. Anorg. Allg. Chem.* **2014**, *640*, 805−813.

(35) Terschüren, H.-U. Untersuchung metallreicher Bariumphosphide und von Erdalkalimetallpnictidchalkogeniden. Ph.D. thesis, University of Kiel, 1989.

(36) Inorganic Crystal Structure Database, ICSD, accessed on-line in April 2015.

(37) Li, B.; Mudring, A.-V.; Corbett, J. D. *Inorg. Chem.* **2003**, *42*, 6940−6945.

(38) Gladyshevskii, E. I.; Fedorov, T. F.; Kuz'ma, Yu.B.; Skolozdra, R. V.; Hladyshevskii, E. I. *Poroshkov. Metallurg.* **1966**, *5*, 305−309.

(39) Bjurström, T.; Arnfelt, H. *Z. Phys. Chem.* **1929**, *4*, 469−476.

(40) Pauling, L. *The Nature of the Chemical Bond*, 3rd ed.; Cornell University Press: Ithaca, NY, 1960.

DOI: 10.1021/acs.inorgchem.5b01253
Inorg. Chem. 2015, 54, 8608−8616

(41) Emmerling, F.; Petri, D.; Röhr, C. *Z. Anorg. Allg. Chem.* **2004**, *630*, 2490−2501.
(42) Fulmer, J.; Kaseman, D.; Dolyniuk, J.; Lee, K.; Sen, S.; Kovnir, K. *Inorg. Chem.* **2013**, *52*, 7061−7067.
(43) Ivanov, A. S.; Boldyrev, A. I.; Frenking, G. *Chem. - Eur. J.* **2014**, *20*, 2431−2435.
(44) (a) *Chemistry, Structure and Bonding of Zintl Phases and Ions*; Kauzlarich, S. M., Ed.; VCH: New York, 1996. (b) Miller, G. J.; Schmidt, M. W.; Wang, F.; You, T.-S. *Struct. Bonding (Berlin)* **2011**, *139*, 1−55.

DOI: 10.1021/acs.inorgchem.5b01253
Inorg. Chem. 2015, 54, 8608−8616